The Equivalent Circuit of Single Crab Muscle Fibers As Determined by Impedance Measurements with Intracellular Electrodes

ROBERT S. EISENBERG

From the Biophysics Department, University College London, England, and the Department of Physiology and Pharmacology, Duke University Medical Center, Durham, North Carolina

ABSTRACT The input impedance of muscle fibers of the crab was determined with microelectrodes over the frequency range 1 cps to 10 kc/sec. Care was taken to analyze, reduce, and correct for capacitive artifact. One dimensional cable theory was used to determine the properties of the equivalent circuit of the membrane admittance, and the errors introduced by the neglect of the three dimensional spread of current are discussed. In seven fibers the equivalent circuit of an element of the membrane admittance must contain a DC path and two capacitances, each in series with a resistance. In two fibers, the element of membrane admittance could be described by one capacitance in parallel with a resistance. In several fibers there was evidence for a third very large capacitance. The values of the elements of the equivalent circuit depend on which of several equivalent circuits is chosen. The circuit (with a minimum number of elements) that was considered most reasonably consistent with the anatomy of the fiber has two branches in parallel: one branch having a resistance R_e in series with a capacitance C_e ; the other branch having a resistance R_b in series with a parallel combination of a resistance R_m and a capacitance C_m . The average circuit values (seven fibers) for this model, treating the fiber as a cylinder of sarcolemma without infoldings or tubular invaginations, are $R_e = 21$ ohm cm^2; $C_e = 47$ μf/cm^2; $R_b = 10.2$ ohm cm^2; $R_m = 173$ ohm cm^2; $C_m = 9.0$ μf/cm^2. The relation of this equivalent circuit and another with a nonminimum number of circuit elements to the fine structure of crab muscle is discussed. In the above equivalent circuit R_m and C_m are attributed to the sarcolemma; R_e and C_e , to the sarcotubular system; and R_b , to the amorphous material found around crab fibers. Estimates of actual surface area of the sarcolemma and sarcotubular system permit the average circuit values to be expressed in terms of unit membrane area. The values so expressed are consistent with the dielectric properties of predominantly lipid membranes.

The values of the specific membrane capacitance of muscle fibers derived from measurements employing step functions of current applied through intracellular electrodes are remarkably large, ranging from 8 μf/cm^2 in frog

(Fatt and Katz, 1951), to 40 $\mu f/cm^2$ in crab (Fatt and Katz, 1953; Atwood, 1963). It is difficult to account for these large values of specific membrane capacitance assuming reasonable dielectric properties of a predominantly lipid sarcolemma. A large underestimate of the surface area of the sarcolemma per unit length of fiber could perhaps account for these large values. Such an underestimate would occur if there were extensive infoldings or invaginations of the sarcolemma, as suggested by Fatt and Katz (1953). Indeed, the apparently large value of membrane capacitance of frog muscle fibers has been attributed in part to the membrane of a sarcotubular system (Falk and Fatt, 1964), the structure of which is discussed by Franzini-Armstrong (1964) and Peachey (1965 *a*). It seemed of interest to see whether the much larger capacitance of crab muscle could also be attributed in greater part to the membranes of a sarcotubular system (first investigated by Veratti (1902) with the light microscope; more recently by Peachey and Huxley (1964) and Peachey (1965 *b*) with the electron microscope).

Electrical measurements can separate the total capacitance of a muscle fiber into different parts only if the time constants of the capacitances and their associated resistances are different. In that case the two capacitances form separate branches of an equivalent circuit which describes the admittance of the membrane structures.

The equivalent circuit of a linear system can most satisfactorily be determined by measuring the impedance of the system to sinusoidal currents of different frequencies; that is, by measuring the relative magnitude and phase of the current and voltage over a range of frequencies. A similar analysis using step functions of current is not possible because of the extraordinary sensitivity of the computed circuit parameters to noise in the potential response (see Lanczos, 1957, p. 279).

Measurements of the phase and magnitude of the input impedance were made over a wide frequency range. The qualitative features of the data showed that the equivalent circuit of the membrane admittance of most crab fibers contained two capacitances, each in series with resistance. Values of the circuit elements were obtained from the best fit of such an equivalent circuit to the experimental data. Finally, the different forms of the equivalent circuit and the values of the circuit elements are discussed in relation to the fine structure of crab muscle fibers.

THEORY

The muscle fiber can be considered as a one dimensional electrical cable. Current injected at a point in the fiber must flow along part of the core resistance before it can pass through the fiber membrane. Since the length of the current path is different for each element of membrane, the value of the core resistance in series with each element of membrane is different. In

such a system the membrane admittance (the AC analog of membrane conductance) is said to be distributed along the core resistance. The validity of this one dimensional model of a cylindrical muscle fiber is discussed in Appendix 3.

The purpose of this investigation is to determine the equivalent circuit of an element of the distributed membrane admittance y [(ohm cm)$^{-1}$]. The only measurements made, however, are those of the input impedance Z (ohms), which is defined here as the ratio of the AC potential to the AC current applied nearby. It is thus necessary to use the equations of cable theory (King, 1965) to relate the properties of the distributed membrane admittance y to those of the observed quantity Z. These equations are (Falk and Fatt, 1964)

$$Z = R + jX = \tfrac{1}{2}(r_i/y)^{\frac{1}{2}} \quad \text{where} \quad y = g + jb, j = (-1)^{\frac{1}{2}} \quad \text{and}$$

$$R = \tfrac{1}{2}(r_i/2g)^{\frac{1}{2}} \frac{([(b/g)^2 + 1]^{\frac{1}{2}} + 1)^{\frac{1}{2}}}{[(b/g)^2 + 1]^{\frac{1}{4}}} \tag{1}$$

$$-X = \tfrac{1}{2}(r_i/2g)^{\frac{1}{2}} \frac{([(b/g)^2 + 1]^{\frac{1}{2}} - 1)^{\frac{1}{2}}}{[(b/g)^2 + 1]^{\frac{1}{4}}}$$

where (1) the input impedance Z has been separated into its in-phase (i.e. real) component R (the input resistance) and its out-of-phase (i.e. imaginary) component X (the input reactance). (2) The distributed membrane admittance y has also been used in component form with real part g (the membrane conductance) and imaginary part b (the membrane susceptance). It should be pointed out that in general R, X, g, and b vary with frequency. (3) r_i is the core resistance per unit length.

An equivalent circuit for an element of the distributed membrane admittance was chosen in the following way. An expression for the admittance, y, of the equivalent circuit being considered was derived by the methods of network analysis (van Valkenburg, 1964) and the input impedance, Z, of a cable with this distributed admittance was calculated by substituting the expression for y in equation (1). The locus of this input impedance (the plot of $-X$ vs. R at many frequencies) was compared with the locus of the input impedance observed experimentally. In this way an equivalent circuit was chosen which gave a good fit to the experimental data.

The circuit values of the more complicated equivalent circuits were chosen by a curve-fitting routine on a digital computer. The computer was programmed to choose those values of the circuit parameters which minimized the deviation (in the mean square sense) of the theoretically computed curve from the experimental data. Because relatively small changes in the value of circuit parameters (say 15%) produce qualitative misfits of the theoretical curve, it is felt that the parameter values are well determined by the impedance measurements.

It is important to remember that the determination of a circuit with a prescribed impedance locus is not unique: there are an infinite number of circuits with more than the minimum number of circuit elements and a large number with the minimum number of elements which have identical impedance loci. One of these circuits has been chosen, the elements of which can be reasonably identified with the anatomical and physical properties of elements of the muscle fiber. The selection of the appropriate circuit is made in the Discussion.

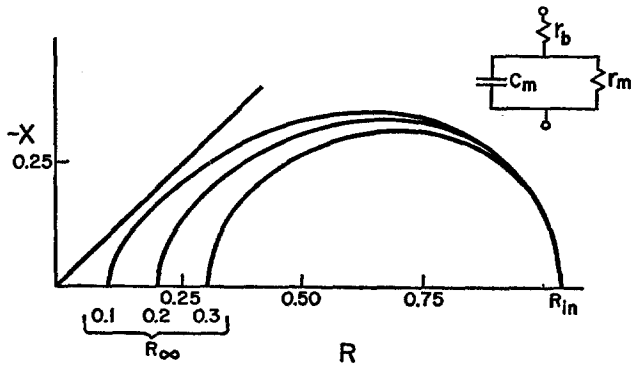

FIGURE 1. Locus of the input impedance of a cable with a one time constant, series resistance membrane admittance. The solid lines are the impedance loci of the cable with the membrane admittance shown. The 45° line represents the limiting high frequency locus for $r_b = 0$; i.e. it represents the limiting behavior for any equivalent circuit of the membrane admittance without series resistance. The numbers enclosed by the brace give the value of R_∞/R_{in} corresponding to each curve. R_∞, the limiting input resistance at high frequency, equals $0.5(r_b r_i)^{\frac{1}{2}}$, where r_i is the internal resistance in ohms/cm. R_{in}, the DC input resistance, equals $0.5\ [(r_m + r_b)\ r_i]^{\frac{1}{2}}$. Thus, $R_\infty/R_{in} = [r/(r + 1)]^{\frac{1}{2}}$ where $r = r_b/r_m$.

Impedance Loci of Equivalent Circuits

Several different circuits of an element of the distributed membrane admittance have been considered. Two of these, the one time constant (Fig. 5, inset) and the two time constant element have been thoroughly discussed by Falk and Fatt (1964). The circuit components will be similarly identified here. Five additional circuits are used.

1. ONE TIME CONSTANT ELEMENT WITH SERIES RESISTANCE

This circuit (Fig. 1) consists of a resistor, r_b, in series with a parallel arrangement of a resistor, r_m, and a capacitor, c_m. The admittance of this element is given by

$$y = \frac{1}{r_m}\left[\frac{(1 + r) + \nu^2 r}{(1 + r)^2 + \nu^2 r^2} + \frac{j\nu}{(1 + r)^2 + \nu^2 r^2}\right] \qquad (2)$$

where the dimensionless variables $r = r_b/r_m$; $\nu = \omega r_m c_m$ have been used. The shape of this impedance locus (Fig. 1) is seen to depend on only one parameter r.

2. TWO TIME CONSTANT ELEMENTS WITH SERIES RESISTANCE

Three such circuits are used. These circuits are equivalent; that is to say, for appropriate values of the circuit elements they have the same resistance and reactance at all frequencies. Fig. 2 shows two of the circuits which have the minimum number of components and Fig. 7 A, a circuit which has more

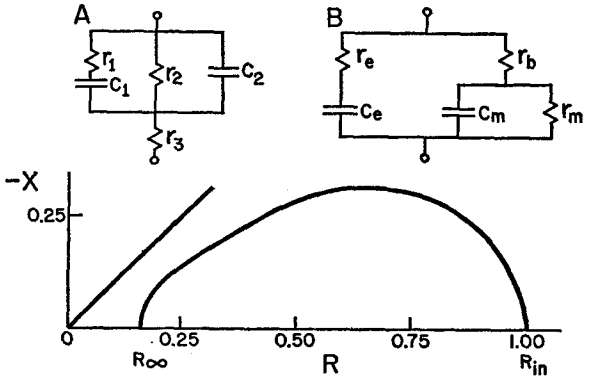

FIGURE 2. Locus of the input impedance of a cable with a two time constant, series resistance membrane admittance. The solid line is a locus of the input impedance of a cable with the membrane admittance A or B. The circuits in A and B contain the minimum number of elements necessary to determine the locus. The locus was calculated for the values $c_2/c_1 = 1.5$; $r_2/r_1 = 2.7$; $r_3/r_2 = 0.024$; $c_1/r_i = 0.72$ μf/megohm. The impedance locus would approach the 45° line through the origin if there were any capacitance without series resistance in the circuits.

than the minimum number of components. An impedance locus for all three equivalent circuits is also shown in Fig. 2. The membrane admittance of the circuit labeled A in Fig. 2 is given by

$$g = \frac{\nu^4 r^2 c^2 (r_3/r_2) + \nu^2\{[r_3/r_2][(1+r)^2 + r^2 c(c+2)] + r + 1\} + r_3/r_2 + 1}{r_2 D}$$

$$b = \frac{\nu^3 rc + \nu r(1+c)}{r_2 D} \qquad (3)$$

with

$$D = \nu^4 (r_3/r_2)^2 r^2 c^2 + \nu^2\{1 + 2(r_3/r_2)(1+r) + (r_3/r_2)^2[r^2(1+c)^2 + 2r + 1]\} + (r_3/r_2 + 1)^2$$

where the dimensionless parameters r_3/r_2, $\nu = \omega r_1 c_1$, $r = r_2/r_1$, and $c = c_2/c_1$ are used.

The shape of this locus depends on three dimensionless parameters and is thus difficult to discuss qualitatively. One important feature of this circuit is its behavior at high frequencies. As $\omega \rightarrow \infty$, the distributed membrane parameters g and b approach $(r_3)^{-1}$ and $(\omega c_2 r_3^2)^{-1}$, respectively. Substitution of these expressions in equations (1) gives the observable properties of the input impedance: R approaches $\frac{1}{2}(r_3 r_i)^{\frac{1}{2}}$, which is called R_∞, and $-X$ first approaches $(4\omega c_2)^{-1}\ (r_i/r_3)^{\frac{1}{2}}$ and then zero. (Neglected terms differ by powers of ω^2.) In other words the resistance remains constant at high frequencies while the reactance varies inversely with frequency. The impedance locus should then approach the real axis at an angle of 90°. This behavior is in contrast to that of models of the membrane admittance without series resistance where the limiting high frequency impedance locus is a 45° line drawn through the origin.

The circuit in Fig. 2 A was that originally used to fit the observed impedance data before the fine structure of crab muscle was known. The elements of the other two circuits (Figs. 2 B and 7 A) can be more reasonably identified with elements of the fine structure of crab muscle. Because the experimental data were analyzed in terms of the circuit in Fig. 2 A, it is necessary to relate the values of the parameters of the other circuits with those in Fig. 2 A. A method of doing this is given in Appendix 1. It should be pointed out here that the circuit in Fig. 7 A has one more circuit element than necessary to determine its impedance locus. The value of the parameters of this circuit cannot be found from impedance measurements (at one pair of terminals) alone but can only be determined if additional assumptions about membrane properties are made.

METHODS

The preparation used in these experiments was the flexor of the carpopodite of the first walking leg of *Portunus depurator* and *Carcinus maenas* bathed in crab Ringer's solution (Fatt and Katz, 1953). The flexor muscle was exposed by removing the shell over the extensor muscle together with the extensor muscle and the limb nerves. The shell beneath the flexor was removed to improve visibility and the muscle was viewed with a stereodissecting microscope by transmitted light.

Micropipettes with resistances of about 4 megohms (measured when dipping into crab Ringer's) were inserted about 40 μ apart into fibers on the exposed surface of the muscle. Microelectrodes used to apply current were filled with 2 M sodium citrate (pH 6) since these passed greater currents than the microelectrodes, filled with 3 M KCl, that were used to record potential. Microelectrodes that showed nonlinearities when passing currents of the order of 10^{-7} amps were rejected. The displacement in membrane potentials was kept smaller than 8 mv in order to remain in the linear region of the muscle current-voltage relation. Records which showed nonlinearities were rejected. Measurements of distance were made using the eyepiece graticule of the microscope.

The setup was similar to that used by Falk and Fatt (1964). Two important differences were the provisions taken to regulate temperature and to minimize capacitive coupling between the electrodes. Because of the large temperature coefficient of membrane resistance in crab muscle (Fatt and Katz, 1953), a semiconductor constant temperature device was used to maintain the muscles at a constant temperature.

To minimize capacitive coupling, a thin aluminum shield, insulated along its bottom edge with plastic film (Saran Wrap), was placed in the Ringer solution between the current and voltage microelectrodes. The plastic film was coated with silicone grease to prevent the formation of a meniscus (which would have increased the capacitance of the microelectrode to the bath) and was driven from the cathode of the recording cathode follower. The reduction in the interelectrode capacitance when the shield touched the fluid was by a factor of between five and ten.

RESULTS

The impedance loci observed showed considerable variation and will be discussed in three groups.

1. The first group of fibers (fibers 1 - 7 in Table I) had impedance loci like those shown in Figs. 3 and 4. The open circles are the raw experimental data. The filled circles are the impedance of the fiber itself after applying the corrections for capacitive artifact discussed in Appendix 2. The frequency at which some of the impedance measurements were made is shown near some points. The frequency at which the other measurements were made can be found, since measurements were taken at constant intervals of log frequency, each frequency being 1.47 times the previous one. Fibers that showed a change of DC input resistance of more than 5% during the course of an experiment were rejected. A 45° line through the origin is shown in these figures since the locus of the input impedance of a cable will approach this line at high frequencies if its distributed membrane admittance includes a capacitance without a series resistance.

The measurements at high frequencies are subject to error. At high frequencies the phase of the observed input impedance tends to be close to 90°. Errors in the measurement of phase by Lissajous figures tend to be rather large under these conditions (Benson and Carter, 1950). Another source of error is systematic error in the corrections for capacitive artifact. This error is analyzed in detail in Appendix 2, where it is shown to be less than 1 kohm in both resistance and reactance at 10 kc/sec.

The solid line is the theoretical locus of the input impedance of a cable with the distributed membrane admittance shown in Fig. 2 A. This is the curve of best fit obtained as described above with a digital computer. The dotted line is the theoretical curve, fitted by eye, for a cable with the distributed admittance shown in Fig. 1. Reference to Figs. 2 and 4 of Falk and Fatt (1964) shows that models of the membrane admittance without a series resistance fail to fit the observed locus; they approach the 45° line through

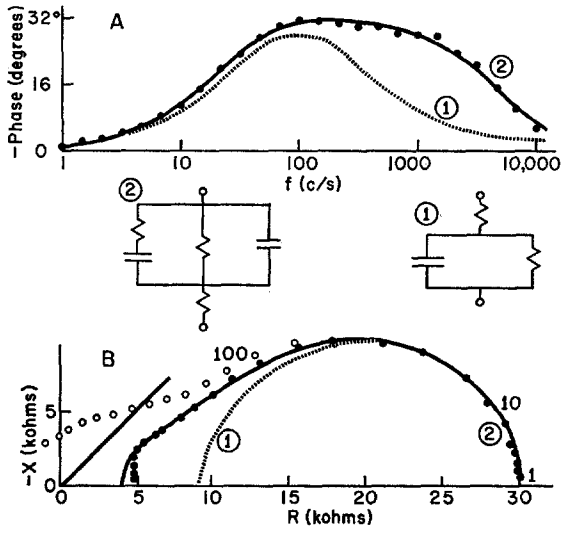

FIGURE 3

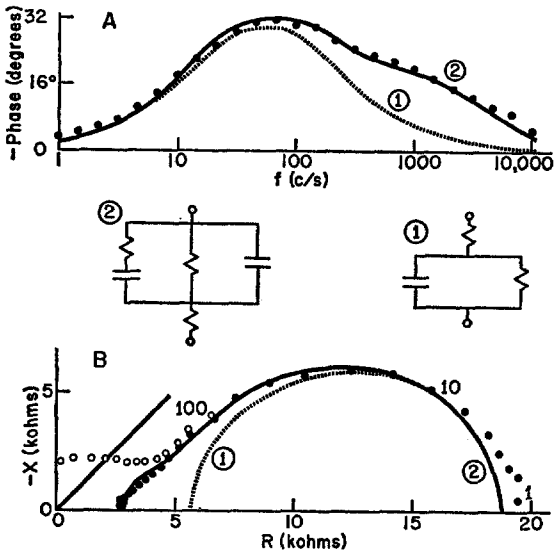

FIGURE 4

FIGURES 3 and 4. Plots of the input impedance of fibers of group 1. A, plot of phase angle of the input impedance against log frequency. The filled circles represent observations corrected for capacitive artifact. The solid line is the "best fit" (determined numerically) for a cable with membrane element (2). The dotted line is the best fit (determined by eye) for a cable with membrane element (1). B, the locus of the input impedance. The open circles represent observations uncorrected for capacitive artifact. The solid line is the locus of the input impedance of a cable with membrane element (2). The dotted line is the locus of the input impedance for a cable with membrane element (1). The frequency at which some of the measurements were made is shown. Fig. 3 shows the properties of fiber 1 (Table I); Fig. 4, the properties of fiber 4 (Table I).

the origin at high frequencies and thus neither intersect the real axis at a finite value nor show a downward bend at high frequencies. Figs. 3 and 4 also include plots of phase angle of the input impedance against log frequency. Only the points that have been corrected for capacitive artifact are shown. The lines are the theoretical curves of best fit, obtained in the manner described above. The phase plot shows a downward trend at frequencies above 400 cps in one case, 100 cps in the other. Only models of the membrane admittance with series resistance give phase plots of the input impedance that decrease with frequency. Since the corrections for capacitive artifact are quite accurate at these frequencies, the downward trend in the phase plot provides good evidence for the presence of a series resistance in the model of the membrane admittance. Models of the membrane admittance containing three capacitances give no better fit.

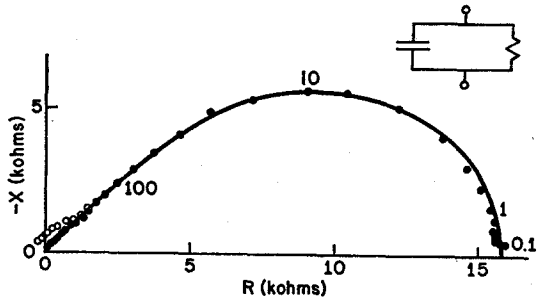

FIGURE 5. The locus of the input impedance of a fiber of group 2. The open circles are points uncorrected for capacitive artifact. The solid line is the impedance locus of a cable with the membrane admittance shown. The fiber whose impedance locus is given here is fiber 2, group 2 (Table I). The frequency at which some of the measurements were made is shown.

2. The impedance locus of one of the two fibers in the second group is shown in Fig. 5. This locus is qualitatively different from those of the first group (see Figs. 3 and 4); the locus is seen to approach a 45° line through the origin at frequencies above 100 cps, and the magnitude of the impedance becomes very small above 1 kc/sec. The solid line represents the input impedance of a cable with a membrane admittance containing one capacitance. More complicated models give no better fit.

3. The input resistances of the fibers of the third group were very low and so the measurements taken at high frequencies were swamped by capacitive artifact and are not shown. At low frequencies, however, a second dispersion (i.e. a second maximum) in the impedance locus could be seen. Fig. 6 shows the input impedance locus at low frequencies of one of the three fibers which unequivocally showed this behavior. There was no indication that these fibers were abnormal; the resting potentials were satisfactory (over 60 mv) and the fibers showed no signs of dissection damage even after many hours.

A potentially serious source of error is the distortion of the impedance loci caused by the assumption of purely one dimensional flow of current. Appendix 3 gives an analysis of this problem and shows that the correction involved

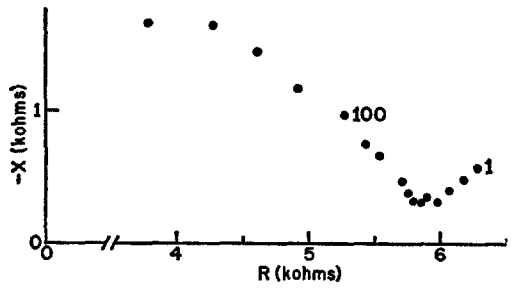

FIGURE 6. The locus of the input impedance of a fiber of group 3. The filled circles represent data uncorrected for capacitive artifact. Note the discontinuity in the abscissa. The frequency at which some of the measurements were made is shown.

TABLE I

CIRCUIT VALUES OF TWO TIME CONSTANT DISTRIBUTED RESISTANCE MODEL

Experiment and genus	R_{in}	R_∞	c_2/c_1	r_2/r_1	r_2/r_2	$\frac{c_1+c_2}{r_i}$	$2a$ or $\begin{cases}2a_1\\2a_2\end{cases}$
	kohms	*kohms*			$\times 10^{-2}$	*μf/megohm*	*μ*
Group 1							
1 *Portunus*	30.1	3.91	1.23	4.50	1.73	1.77	(365)
2 *Portunus*	23.7	2.84	0.67	13.5	1.48	4.34	(192)
3 *Portunus*	36.6	13.8	0.49	2.44	16.5	1.00	87*
4 *Carcinus*	18.5	2.76	0.74	10.6	2.28	8.60	(198)
5 *Carcinus*	28.0	5.50	0.19	8.96	3.95	4.62	{122 81*
6 *Carcinus*	23.4	—	0.23	23.9	—	9.96	116*
7 *Carcinus*	11.7	0.44	0.52	8.56	1.38	16.5	172
Group 2							
1 *Carcinus*	20.7	—	—	—	—	16.1	(167)
2 *Carcinus*	15.5	—	—	—	—	33.6	(182)

Braces enclose the major and minor axes as discussed in the text.
Parentheses enclose measured diameters which could not be checked for agreement with internal resistivity of R_i = 58 ohm-cm because no space constant was measured.
* Calculated; not a measured diameter.

does not account for the shape of the impedance loci of the fibers in group 1. However, in two fibers of this group (Nos. 6 and 7 in Tables I and II) the input resistance at high frequencies was small enough so that the effect of three dimensional spread of current was considerable.

Evaluation of Circuit Parameters

The values of the circuit elements (circuit parameters) of the two time constant series resistance model (shown in Fig. 2 A) that best fit the corrected experimental measurements are given in Table I. R_{in} and R_∞ are the input resistance observed at zero and infinite frequencies respectively. The diameters of the fibers marked with an asterisk were calculated by the method of Fatt and Katz (1951) from an average value of the volume resistivity of the core material (myoplasm) of 58 ohm cm² (Atwood, 1963), assuming the fibers to be circular in cross-section. If the radius so calculated was not in reasonable agreement with the radius observed, the fiber was assumed to be elliptical in cross-section, the major axis being the observed diameter, the minor axis being computed from the internal resistivity. The second group of fibers in Table I are those which a one time constant model adequately described.

TABLE II

CIRCUIT VALUES REFERRED TO OUTER SURFACE AREA

Experiment and genus	λ^*	$C_1 + C_2$	C_1	C_2	R_1	R_2	R_1
	μ	$\mu f/cm^2$	$\mu f/cm^2$	$\mu f/cm^2$	ohm-cm²	ohm-cm²	ohm-cm²
3 *Portunus*	743	36	24	12	21	128	52
5 *Carcinus*	750	108	91	17	5.1	129	14
6 *Carcinus*	851	150	122	28	—	146	6.1
7 *Carcinus*	935	75	50	25	0.16	113	13.2

*λ is the DC space constant.

Parameters for a unit length of fiber can be found if one additional quantity, the DC space constant, is known. In four of the seven fibers of the first group the space constant was determined by measuring the input resistance at a known electrode separation (Table II). In the other fibers loss of resting potential and input resistance upon removal or reinsertion of the microelectrode made an accurate determination impossible. Knowledge of the cross-sectional area and circumference of the fibers allows the parameters to be referred to the surface area of a cylinder of those dimensions. The resulting parameters give the properties of a hypothetical sarcolemma, one that would surround the outer surface of the fiber without infoldings or tubular invaginations. It is necessary to estimate the surface area of these different systems of sarcolemma (infoldings and tubules, see Peachey, 1965 *b*) in order to refer the circuit parameters to the areas of those structures in which they presumably arise. This problem is treated further in the Discussion.

The data from the three fibers for which the space constant was not determined can be included in average values of the parameters by the procedure

of Falk and Fatt (1964, p. 97). Although this procedure assumes that the fiber parameters are all independent of fiber radius whereas the anatomical data suggest that they should be linear functions of the radius, the effect of this assumption on the values calculated is smaller than 25%. The average values of the dimensionless ratios are less sensitive to such assumptions. The average values so computed for the fibers in group 1 for the circuit in Fig. 2 A are: C_2 = 18.9 μf/cm^2; C_1 = 40.2 μf/cm^2; R_2 = 176 ohm cm^2; R_1 = 16.9 ohm cm^2; R_3 = 6.9 ohm cm^2; C_2/C_1 = 0.47; R_2/R_1 = 10.4; R_2/R_3 = 25.5. It must be pointed out that the surface area implicit in these values is that of a simple cylinder of sarcolemma without invaginations or infoldings.

DISCUSSION

Previous studies of the linear electrical properties of crab muscle (Fatt and Katz, 1953; Atwood, 1963) have used square pulse (transient) analysis. Because of the difficulties in separating time constants of comparable magnitude with this technique (Lanczos, 1957, p. 279), it is not surprising that previous investigations did not find evidence for the existence of a two time constant membrane element. The presence of a resistance in series with both capacitances of the membrane circuit element would also be difficult to reveal with transient response methods since the initial jump in potential across the series resistance would be obscured by the uncorrected capacitive artifact.

To choose one equivalent circuit from the many possible circuits, the fine structure of crab muscle fibers must be considered. When such an equivalent circuit is chosen it becomes possible to refer the values of the circuit elements to the surface area of the structures in which they are supposed to arise. It is possible to test the validity of the choice of equivalent circuit by comparing the size of these specific capacitances with those expected from predominantly lipid membranes.

The basic features of the fine structure of crab (*Carcinus maenas*) muscle are described by Peachey and Huxley (1964) and Peachey (1965 *b*). The muscle fibers have deep clefts formed by gross infolding of the fiber surface. Two types of tubular invaginations of the plasma membrane extend from both these clefts and the outer surface. One set of tubules is associated with the *Z* lines and seems to have no direct connection with excitation-contraction coupling. The other set of tubules is associated with the boundary between the *A* and *I* bands and forms "dyadic" structures with parts of the sarcoplasmic reticulum, these tubules being implicated in excitation-contraction coupling. An amorphous material surrounds the fiber and fills the clefts.

The simplified equivalent circuit that one might expect from such an arrangement of membranes is shown in Fig. 7 A. This circuit is simplified in two ways: first, the distributed membrane admittance of all the tubules is

lumped into one set of elements R_{ce}, C_e in series with the tubular core resistance R_e; second, the distributed admittance of the sarcolemma of the clefts is lumped with the admittance of the sarcolemma of the outer surface (the lumped elements being R_m, C_m), and both are considered to be in series with one resistance, R_b, arising in the amorphous material. While these approximations have been made to avoid considerable arbitrary complication in the analysis, the assumptions involved are not likely to introduce gross errors into the following discussion.

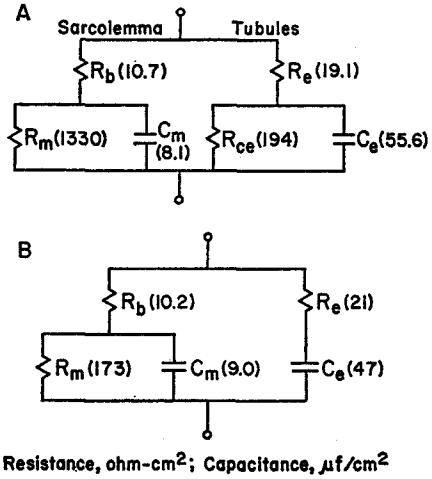

FIGURE 7. Two equivalent circuits. Circuits A and B have the same resistance and retance at all frequencies (for the circuit values indicated). Note that B contains the minimum number of circuit elements necessary to describe its admittance. The circuit A thus has one redundant element. The branches of the circuits are labeled to show the structures of the muscle fiber in which they are presumed to arise. The numbers in parentheses are the average circuit values computed assuming $R_{ce}C_e = R_mC_m$ (in A) and (in B) $R_{ce} = \infty$. These numbers represent the characteristics of a hypothetical membrane without infoldings or tubular invaginations.

It is possible that the observed low frequency dispersion could be produced by one of the capacitances shown in Fig. 7 A. It is more likely, however, that this dispersion arises from some diffusion process since the membrane capacitance necessary to explain the low natural frequency of this dispersion would be very large (see the discussion of a similar large capacitance in Fatt, 1964). It is possible that the fibers with only one capacitance belong to a second population of fibers analogous to those found in other limb muscles of the crab by Atwood, Hoyle, and Smyth (1965); Dorai Raj (1964); Cohen (1963); and Atwood (1963); this second type of fibers might be expected to have a different fine structure from that described by Peachey and Huxley (1964) and Peachey (1965 *b*).

The values of the circuit elements in the circuit in Fig. 7 A cannot be determined from the average values previously calculated since there is a redundant element (R_{ce} or R_m) in this circuit. Only by making some assumption about the size of this element can circuit values be derived. Two such assumptions are made here, each resulting in a set of different circuit values. In one case the resistance, R_{ce}, of the tubular membrane is assumed to be very high. The circuit and circuit values resulting from this assumption are shown in Fig. 7 B. Details of the calculation can be found in Appendix 1.

In the second case the sarcolemma and the tubular membranes are assumed to have similar electrical properties, that is to say the time constants $R_{ce}C_e$ and R_mC_m are set equal. The values calculated (see Appendix 1) on this assumption are shown in Fig. 7 A.

It is of interest to refer these latter values to the areas of the structures from which they are supposed to arise, using the estimates of these areas given by Peachey and Huxley[1] (also see Peachey, 1965 *b*). Using the circuit of Fig. 7 A, the value of "C_e" (now referred to the actual area of the tubular membrane) is 1.6 μf/cm^2 and that of "C_m" (referred to the actual area of the sarcolemma) is 4.5 μf/cm^2 (for the average fiber radius of 64 μ). The first number is what would be expected for a predominantly lipid membrane; the second number is some three times too large. Since there are large errors involved in the microscopic measurements of the surface area of the clefts and in the electrical determination of C_m, this value is considered satisfactory.

Appendix 1

Equivalence Relations

In this section a method is developed for finding the relations between the circuit values of the components of equivalent circuits. The method developed is applicable to circuits of arbitrary complication and is more practical than the classical methods involving the simultaneous solution of several, usually quadratic, equations (Starr, 1938). The particular set of equations derived here gives the parameters of the non-minimum resistance circuit shown in Fig. 7 A in terms of the parameters of the minimum resistance circuit shown in Fig. 2 A.

The impedance function of the circuit shown in Fig. 2 A is known (equation 3), so that the problem of finding the equivalence relations reduces to that of synthesizing a network of given configuration (in this case that of Fig. 7 A) from the known impedance function. The approach to such a problem is developed in the theory of network synthesis (van Valkenburg, 1960).

The admittance of the circuit of Fig. 2 A can be written as

$$y = \frac{(s - N_1)(s - N_2)}{R_8(s - D_1)(s - D_2)}$$

[1] Personal communication.

(where the symbols are defined in equations (6) that follow). This function can be derived from that given in equation (3) by substituting the frequency variable s for the frequency variable $j\omega$ and then factoring both the numerator and denominator of the resulting function. This expression for y is divided on both sides by s to make the following expansion into partial fractions possible (symbols defined in equations 6)

$$\frac{y(s)}{s} = \frac{J}{s} + \frac{K}{s - D_1} + \frac{L}{s - D_2}$$

The first term on the right-hand side of the above equation specifies the DC behavior of the circuits. Since the circuit being synthesized contains two DC paths, it is necessary to break this term into two parts, one corresponding to each path

$$y(s) = (1 - \theta)\, J + \frac{Ks}{s - D_1} + \theta J + \frac{Ls}{s - D_2} \tag{4 a}$$

$$= \frac{-(1 - \theta)JD_1 + s[(1 - \theta)J + K]}{s - D_1} + \frac{-\theta JD_2 + s[\theta J + L]}{s - D_2} \quad 0 \leq \theta \leq 1 \tag{4 b}$$

The value of the parameter θ will be determined by the value that is assumed for the ratio R_{ce}/R_m. One such assumption, that $R_{ce} = \infty$ (i.e., $\theta = 1$), gives the circuit of Fig. 7 B. The synthesis of a circuit with the minimum number of elements (e.g., the circuit of Fig. 7 B) does not require this splitting of a term of the impedance function.

In order to complete the derivation of the equivalence relations it is simply necessary to write the admittance of the circuit being synthesized and compare this admittance with that given in equation (4). Since the circuit in Fig. 7 A contains two parallel branches, the admittance of each branch can be identified with one of the terms of the right-hand side of equation (4 *b*). The admittance of the branch containing R_e, C_e, and R_{ce} is

$$\frac{1}{R_e + [sC_e + 1/R_{ce}]^{-1}} = \frac{[R_{ce}\, R_e\, C_e]^{-1} + sR_e^{-1}}{s + [R_e + R_{ce}][R_{ce}\, C_e\, R_e]^{-1}} \tag{5}$$

The equivalence relations for this branch can most easily be found by examining the behavior of equation (5) and the corresponding term of equation (4 *b*) at the extremes of frequency. The rest of the equivalence relations can be found by applying the same procedure to the second term on the right-hand side of equation (4 *b*) and to the branch of the circuit of Fig. 7 A containing R_m, C_m, and R_b.

The resulting expressions are:

$$R_e = \frac{1}{K + (1 - \theta)J} \qquad C_e = \frac{-[K + (1 - \theta)J]^2}{KD_1}$$

$$R_b = \frac{1}{\theta J + L} \qquad R_m = \frac{L}{\theta J(\theta J + L)}$$

$$C_m = \frac{-(\theta J + L)^2}{LD_2} \qquad R_{ce} = \frac{K}{(1 - \theta)J(K + [1 - \theta]J)}$$

with

$$K = \frac{(D_1 - N_1)(D_1 - N_2)}{R_3 D_1(D_1 - D_2)} \qquad J = \frac{N_1 N_2}{R_3 D_1 D_2}$$

$$L = \frac{(D_2 - N_1)(D_2 - N_2)}{R_3 D_2(D_2 - D_1)} \qquad N_{1,2} = \frac{-B \pm [B^2 - 4A]^{\frac{1}{2}}}{2A} \tag{6}$$

$$D_{1,2} = \frac{-Q \pm [Q^2 - 4FG]^{\frac{1}{2}}}{2G}$$

$$A = R_1 R_2 C_1 C_2 \qquad B = R_1 C_1 + R_2 C_2 + R_2 C_1$$

$$F = R_3 + R_2 \qquad G = R_1 R_2 R_3 C_1 C_2$$

$$Q = R_1 R_2 C_1 + R_3 [R_1 C_1 + R_2 C_2 + R_2 C_1]$$

The two assumptions concerning the circuit of Fig. 7 A that are used here set specific values for the parameter, θ. The assumption that R_{ce} be infinite sets $\theta = 1$. The other assumption directly sets $R_{ce}C_e = R_mC_m$, which relation implicitly sets the value of θ. The equation resulting from the substitution of the appropriate relations from (6) into this latter expression gives:

$$\theta = \frac{-W + [W^2 - 4YX]^{\frac{1}{2}}}{2X}$$

$$W = J^2(D_1 - D_2) - J(LD_1 + KD_2)$$

$$X = J^2(D_2 - D_1)$$

$$Y = LD_1J$$

The value of θ determined by these assumptions is then substituted into the expressions (6), thus giving a well determined set of equivalence relations. These equivalence relations have been verified by computing the impedance function of the circuit shown in Fig. 7 A, substituting the relations (6), and checking that the result is the impedance function of the circuit in Fig. 2 A.

All the equivalence relations derived above have an inherent ambiguity since the symmetry of the circuit shown in Fig. 7 A makes the two parallel branches indistinguishable. This ambiguity makes it impossible to tell whether the larger capacitance should be called C_e or C_m.

Appendix 2

Corrections for Capacitive Artifact

The corrections for capacitive artifact (see Fig. 8) are calculated from the equations given by Falk and Fatt (1964). Their derivation can be found in Eisenberg (1965).

$$R = R_{obs}[1 - \omega^2(C_1 + C_2)C_3R_VR_I] - X_{obs}\omega[R_V(C_1 + C_2) + C_3R_I] - \omega^2C_1C_3R_VR_IR_{mon} \quad (7a)$$

$$-X = -X_{obs}[1 - \omega^2(C_1 + C_2)C_3R_VR_I] - R_{obs}\omega[R_V(C_1 + C_2) + C_3R_I] + \omega R_V[C_4R_I - C_1R_{mon}] \quad (7b)$$

R_{obs} and $-X_{obs}$ are the observed input resistance and reactance at frequency $f = \omega/2\pi$, R and $-X$ are the actual input resistance and reactance of the fiber at that frequency. R_V and R_I are the resistances of the voltage and current electrode, respectively; R_{mon} is the resistance of the monitor resistance used to measure current; the stray capacitances are defined in Fig. 8. All capacitances are in farads; all resistances and reactances, in ohms.

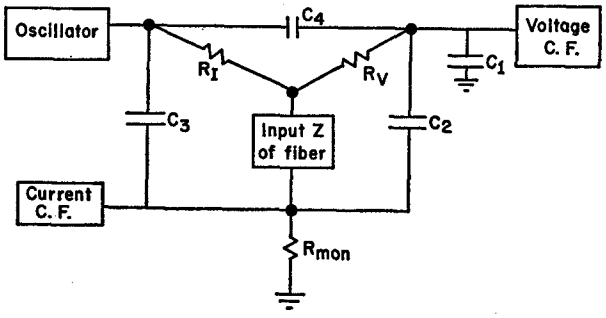

FIGURE 8. Equivalent circuit of setup showing significant stray capacitances. *C.F.* means cathode follower. The resistances are identified in the text. C_1 is the capacitance from the voltage microelectrode to ground. C_2 and C_3 are, respectively, the capacitances from the voltage, and current, microelectrodes to the Ringer solution. C_4 is the coupling capacitance between the microelectrodes.

These equations have a very important property; the correction for capacitive artifact itself depends on the impedance being observed. Thus, any technique for correcting the observed impedance for artifact must itself measure that impedance. Since the electronic measurement of impedance is difficult, electronic compensation is not practicable (see the attempt by Pugsley, 1963). It is not even possible to use electronic compensation networks at low frequencies where the artifact is not so large (below 3 kc/sec) since the largest term in the corrections at low frequencies is the one which depends on the observed impedance. Two simpler methods of correcting for capacitive artifact must also be rejected. It is not possible to set the values of the stray capacitances so that the artifact disappears. Even if this were practical at one frequency, the variation of R and $-X$ with frequency ensures that the artifact would not vanish at another frequency. Second, the solution of equations (7) for R_{obs} and $-X_{obs}$ as a function of R and $-X$ (Eisenberg, 1965) shows that the subtraction of the impedance observed with the current electrode outside the muscle fiber from that observed with the current electrode inside the fiber will not give R and $-X$.

The error in the corrections and thus much of the systematic error in R and $-X$ is determined by the errors in the quantities from which they are calculated; that is, by the errors in the values of the stray capacitances. The error in R can be calculated by taking the total differential (Widder, 1961) of equation (7 *a*). If the following numerical estimates of the parameters are made:
$R_V = R_I = 5$ megohms; $C_1 = 1.0$ *pf*; $C_2 = C_3 = 2$ *pf*; $C_4 = 0.001$ *pf*; $R_{mon} = 10$ kohms; $R_{obs} = -X_{obs} = 1$ kohm (at 10 kc/sec); and if the errors in measurement are assumed to be $\delta C_1 = \delta C_3 = 0.1$ *pf*; $\delta C_2 = 0.3$ *pf*; $\delta(-X_{obs}) = 100$ ohms; $\delta R_{obs} = 500$ ohms; $\delta R_V = \delta R_I = 0$; then the total error in R (at 10 kc/sec) is calculated to be 700 ohms.

The calculation of the error $-X$ is more complicated since one of the parameters in equation (7 *b*), namely C_4 (the interelectrode capacitance), was measured by an indirect method. Immediately after a series of records had been taken from a fiber, the current electrode was removed so that it was just outside the fiber; measurements of the apparent input impedance produced by the stray capacitances were made at different frequencies. The value of the fiber reactance $-X$ is then zero, so equation (7 *b*) can be solved for C_4 in terms of R_{obs}, $-X_{obs}$, and the other circuit parameters. Some test of the validity of the above procedure is provided by calculating C_4 at different frequencies. If the above method is correct, the calculated value of C_4 should be the same at different frequencies. It remains constant within the estimated error of phase measurement (15%) under these conditions.

Because the equation for $-X$ involves a quantity which is itself a calculated quantity (C_4), the following procedure was used to estimate the error in $-X$. The total differential of C_4 was taken, regarding C_4 as a function of the other stray capacitances. This expression for the error in C_4 was then used in the expression for the error in $-X$ (the total differential of $-X$). The results show that those terms involving quantities which do not change when the current electrode is withdrawn from the fiber cancel completely. All the error in $-X$ is thus caused by the *changes* in the values of R_{obs}, $-X_{obs}$, and R_I that occur when the current electrode is removed from the muscle fiber. When the same estimates given above are used (and assuming that outside the fiber $R_{obs} = -X_{obs} = 0$, $R_I = 7$ megohms) the total error in $-X$ is about 600 ohms. The cancellation of terms in the expression for the error in $-X$, which may at first seem surprising, is physically reasonable since this method of "measuring" C_4 results in a quasi-differential measurement of $-X$; i.e. it "subtracts off" most of the errors. The analytical expressions for the residual error are given in Eisenberg (1965).

Appendix 3

Errors in One Dimensional Cable Theory

The major error in the treatment of a cylindrical muscle fiber as a one dimensional cable arises because of the neglect of the three dimensional spread of current.

The equations describing the potential within a cylinder with a thin high impedance coating, current being applied from a point source just under the coating and the external medium taken as isopotential, are presented in Falk and Fatt (1964).

$$Z_{cyl} = \tfrac{1}{2} r_i\, a \sum_{n=-\infty}^{\infty} \cos n\theta \sum_{\beta} \frac{\beta \exp(-\beta x/a)}{\beta^2 - n^2 + 0.25(r_i\, y)^2 a^4} \qquad (8)$$

where β are the roots (in general complex) with positive real parts of

$$\beta \frac{J_{n-1}(\beta)}{J_n(\beta)} = n - 0.5\, a^2 r_i\, y \qquad n = \cdots -2, -1, 0, 1, 2 \cdots \qquad (9)$$

θ is the circumferential angular coordinate of the point at which potential is measured.

x is the distance along the fiber axis (the axial coordinate) of the point at which potential is measured.

$J_n(\beta)$ is the Bessel function of the first kind, order n, of argument β (Watson, 1962).

The primary difficulty in using this solution is that involved in finding the roots β of the expression (9). The following rules proved useful: (1) the smallest root for $n = 0$, β either real or complex, was found to be well approximated by $a(r_i y)^{1/2}$ (the reciprocal of the complex space constant in dimensionless units) where as before r_i is the internal resistance in ohms/cm and y is the distributed membrane admittance in (ohm cm)$^{-1}$; a is the fiber radius in cm; (2) The other roots for $n = 0$, the roots being real or complex, lie very close to the poles (infinities) of the real function $x[J_o(x)]/J_1(x)$. This latter function is tabulated in Onoe (1958). (3) The rest of the roots, i.e. those for $n \neq 0$, either real or complex, lie very close to the roots of $J_n'(\beta)$. The roots of this latter function, the prime denoting differentiation with respect to β, are well known (Watson, 1962). An explanation of these rules is given in Eisenberg (1965).

In order to estimate the error in the results caused by the three dimensional spread of current some model of the membrane admittance must be used. The model of the membrane admittance used in these calculations will be the two time constant model without a resistance in series with both capacitances. The results of the calculation will show to what extent three dimensional effects make the impedance locus of a fiber without a series resistance in the membrane element look like a fiber with a series resistance in the membrane element.

The particular fiber, the behavior of which is analyzed here, is assumed to have the characteristics $R_i = 50.2$ ohm cm; $R_m = 725$ ohm cm^2; $a = 80\ \mu$; $C_m = 5\ \mu f/\text{cm}^2$. These give the observable DC characteristics: $R_{cable} = 30$ kohms; space constant, 2.4 mm. The observable characteristics at high frequency (10 kc/sec) are $-X_{cable} = R_{cable} = 1$ kohm; the frequency-dependent space constant (the reciprocal of the real part of $(r_i y)^{1/2}$) is 225 μ. R_{cable}, $-X_{cable}$ represent the impedance of a fiber in which the electrodes are at zero separation. All the current at 10 kc/sec is assumed to leave the fiber through the membrane capacitance C_m.

Table III shows the input impedance, computed for an electrode separation of $x = 0.5\ a = 40\ \mu$ ($\theta = 0^0$), for the three dimensional cylinder (R_{cyl}, $-X_{cyl}$). In these experiments measurements were actually made of the impedance of a cylinder, namely the muscle fiber, so that R_{cyl}, $-X_{cyl}$ correspond to the observed points. The theoretical curves were calculated, however, by one dimensional cable theory, as-

suming the electrodes were at zero separation. Thus the calculated points correspond to R_{cable}, $-X_{\text{cable}}$. If the theoretical curves had been calculated from one dimensional cable theory, using the actual electrode separation (from equation 3 of Falk and Fatt), the error involved would have been larger. $R(x)$, $-X(x)$ in Table III give the input impedance for an electrode separation of $x = 40$ μ. Since the decrement of potential caused by the electrode separation acts in the opposite direction from the increment in potential caused by the convergence of current near a point source, the two errors tend to cancel one another.

Table III shows that the error in the input reactance at high frequency ($-X_{\text{cyl}} - (-X_{\text{cable}})$) is in the wrong direction to explain the downward bend of the impedance locus at high frequencies: the three dimensional effects would make the observed reactance larger than that calculated from a one dimensional model. The

TABLE III

EFFECTS OF THREE DIMENSIONAL SPREAD OF CURRENT

Parameter	Low frequency	High frequency
	DC	*10 kc/s*
$(r_i y)^{1/2} a$	0.034	$0.356(1 + j)$
R_{cable}	30.00	1.00
$-X_{\text{cable}}$	—	1.00
$R(x)$	29.49	0.84
$-X(x)$	—	0.84
R_{cyl}	30.63	1.96
$-X_{\text{cyl}}$	—	1.48
$R_{\text{cyl}} - R_{\text{cable}}$	0.63	0.96
$-X_{\text{cyl}} - (-X_{\text{cable}})$	—	0.48

Units of all impedances are kohms.
Symbols defined in text.

error in the input resistance ($R_{\text{cyl}} - R_{\text{cable}}$), caused by the convergence of current near a point source, is about the same at the two frequencies and produces a shift to the right of the impedance locus of about 0.6 kohm. This shift is in the right direction but is not large enough to account for the input resistance observed at high frequencies.

The shift is large enough to introduce some error into the measurement of r_b and thus c_m (which is partly determined by the time constant $r_b c_m$) but does not change the qualitative interpretation of the results. If the electrodes were only 16 μ apart, say, the contribution to the observed input resistance at high frequencies would have been much greater, about 6 kohms. For this reason it was important to keep the electrodes about 40 μ apart.

The large value of the input resistance at high frequencies that was found in one fiber (13.8 kohms in fiber 3 of Tables I and II) is evidence that this resistance is not caused by the three dimensional spread of current. The large value of this resistance can be accounted for by three dimensional effects only if the electrodes were less than 10 μ apart. However, since dimpling of the fiber membrane around the microelectrodes (which is very pronounced in this preparation), angular displacement of

the electrodes, and the presence of infoldings of the plasma membrane between electrodes would make the electrodes further apart than they seemed, it is unlikely that the electrodes were as little as 25 μ apart.

It is a pleasure to thank G. Falk, P. Fatt, A. F. Huxley, L. D. Peachey, and E. A. Johnson for many helpful discussions.

Received for publication 2 December 1966.

REFERENCES

ATWOOD, H. L. 1963. Differences in muscle fibre properties as a factor in "fast" and "slow" contraction in *Carcinus*. *Comp. Biochem. Physiol.* **10**: 17.

ATWOOD, H. L., G. HOYLE, and T. SMYTH, JR. 1965. Responses of crab-muscle fibers. *J. Physiol, (London)*. **180**: 449.

BENSON, F. A., and A. O. CARTER. 1950. A critical survey of some phase angle measurements using a cathode-ray tube. *Electron. Eng.* **22**: 238.

COHEN, M. J. 1963. Crustacean muscle and nerve. *Quart. J. Microscop. Sci.* **104**: 551.

DORAI RAJ, B. S. 1964. Diversity of crab muscle fibers. *J. Cellular Comp. Physiol.* **64**: 41.

EISENBERG, R. S. 1965. A.C. Impedance of Single Muscle Fibres. Ph.D. Thesis in Biophysics, University of London.

FALK, G., and P. FATT. 1964. Linear electrical properties of striated muscle fibres observed with intracellular electrodes. *Proc. Roy. Soc. (London), Ser. B.* **160**: 69.

FATT, P. 1964. Analysis of the transverse electrical impedance of striated muscle. *Proc. Roy. Soc. (London), Ser. B.* **159**: 606.

FATT, P., and B. KATZ. 1951. An analysis of the end-plate potential recorded with an intra-cellular electrode. *J. Physiol., (London)*. **115**: 320.

FATT, P., and B. KATZ. 1953. Electrical properties of crustacean muscle fibres. *J. Physiol., (London)*. **120**: 171.

FRANZINI-ARMSTRONG, C. 1964. Fine structure of sarcoplasmic reticulum and transverse tubular system in muscle fibres. *Federation Proc.* **23**: 887.

KING, R. W. 1965. Transmission Line Theory. Dover Publications, Inc., New York.

LANCZOS, C. 1957. Applied Analysis. Pitman Medical Publishing Co., Ltd., London.

ONOE, M. 1958. Tables of Modified Quotients of Bessel Functions of the First Kind for Real and Imaginary Arguments. New York, Columbia University Press.

PEACHEY, L. D. 1965 *a*. The sarcoplasmic reticulum and transverse tubules of the frog's sartorius. *J. Cell Biol.* **25**(3, Pt. 2): 209.

PEACHEY, L. D. 1965 *b*. Excitation contraction coupling in striated muscle. *Federation Proc.* **24**: 1124.

PEACHEY, L. D., and A. F. HUXLEY. 1964. Transverse tubules in crab muscle. *J. Cell Biol.* **23**(2): 70A.

PUGSLEY, I. D. 1963. Microelectrode measurements of membrane resistance and capacitance in the sartorius muscle of the toad. *Australian J. Exp. Biol. and Med. Sc.* **41**: 615.

STARR, A. T. 1938. Electric Circuits and Wave Filters. Pitman Medical Publishing Co., Ltd., London, 2nd edition.

VAN VALKENBURG, M. E. 1960. Network Synthesis. John Wiley & Sons, Inc., New York.

VAN VALKENBURG, M. E. 1964. Network Analysis. Prentice-Hall, Inc., Englewood Cliffs, N. J. 2nd edition.

VERATTI, E. 1902. Investigations on the fine structure of striated muscle fiber. *Mem. Reale Inst. Lombardo.* **19:** 87, No. 10 of Series III. Reprinted in English translation in *J. Biophys. Biochem. Cytol.* **10**(4, Pt. 2): 1.

WATSON, G. N. (1962). Treatise on the Theory of Bessel Functions. Cambridge University Press, London. 2nd edition.

WIDDER, D. V. 1961. Advanced Calculus. Prentice-Hall, Inc., London. 2nd edition.